

RSC Advances



This is an *Accepted Manuscript*, which has been through the Royal Society of Chemistry peer review process and has been accepted for publication.

Accepted Manuscripts are published online shortly after acceptance, before technical editing, formatting and proof reading. Using this free service, authors can make their results available to the community, in citable form, before we publish the edited article. This *Accepted Manuscript* will be replaced by the edited, formatted and paginated article as soon as this is available.

You can find more information about *Accepted Manuscripts* in the [Information for Authors](#).

Please note that technical editing may introduce minor changes to the text and/or graphics, which may alter content. The journal's standard [Terms & Conditions](#) and the [Ethical guidelines](#) still apply. In no event shall the Royal Society of Chemistry be held responsible for any errors or omissions in this *Accepted Manuscript* or any consequences arising from the use of any information it contains.

Nano-channels array etched in hexagonal boron nitride meso-membranes by focused ion beam.[†]

S. Linas,^a R. Fulcrand,^b F. Cauwet,^a B. Poinso^t and A. Brioude.^{*a}

Received Xth XXXXXXXXXXXX 20XX, Accepted Xth XXXXXXXXXXXX 20XX

First published on the web Xth XXXXXXXXXXXX 200X

DOI: 10.1039/b000000x

Meso-membranes with highly ordered nano-channels array have been fabricated by patterning hexagonal boron nitride (h-BN) films using focused ion beam. The complete experimental procedure is given in details from the chemical vapor deposition for h-BN synthesis to its patterning and the final membrane design for nano-fluidic experiments. The membranes obtained are characterized at each experimental step by electron microscopy and Raman spectroscopy. The technique is finally applied to fabricate devices in which the only passage for a fluid is a nanochannels array etched in a h-BN film.

Confinement of fluids in channels is a versatile topic involved in promising applications such as energy generation,¹ ultra-filtration^{2,3} including water purification⁴ and desalination,⁵ DNA sequencing,^{6–8} chemical synthesis⁹ or microbial fuel cells.¹⁰ As the fluid confinement reaches the nano-scale, new phenomena arise and the nature of the walls of the channels gain more and more influence on the behavior of the fluid. Experimentally, nanotubes are an ideal nano-object for nanofluidics, offering channels from few to tens of nanometers in diameter over micrometer length-scale.^{11–15}

Compared to carbon nanotubes (CNTs), boron nitride nanotubes (BNNTs) possess many advantages such as an improved chemical stability¹⁶, better biocompatibility¹⁷ or a resistance to oxidation at high temperature.^{18,19} Highlighting the importance of the nature of the walls of the channels, BNNT are seen to be superior to CNT for nanofluidic applications: molecular dynamics calculations suggest that waters flows through BNNT of smaller diameter than CNT²⁰ and BNNT are also predicted to transport water while rejecting salt.²¹ Due to a giant surface charge, BN is a good candidate for conversion of osmotic energy. A very recent experiment for single BNNTs have shown that the osmotic energy conversion reaches power density in the order of kW.m⁻²,²² exceeding by several orders of magnitude the power density of other exchange membranes.¹

These extremely encouraging results concerning BN based membranes concern samples that are hardly producible at large scale (e.g. 10¹⁰ BNNT.cm⁻²). In order to benefit from the superior properties of BN while producing large-scale and high density membranes, we propose to use a thin hexagonal boron nitride (h-BN) film patterned by focused ion beam (FIB)²³ to etch

[†] Electronic Supplementary Information (ESI) available: time evolution of membranes exposed to air. See DOI: 10.1039/b000000x/

^a LMI, Univ. Lyon 1 and CNRS UMR5615, 43 Bd du 11 Novembre 1918, 69622 Villeurbanne Cedex, France.

^b ILM, Univ. Lyon 1 and CNRS UMR5306, 10 Rue Ada Byron, 69622 Villeurbanne Cedex, France.

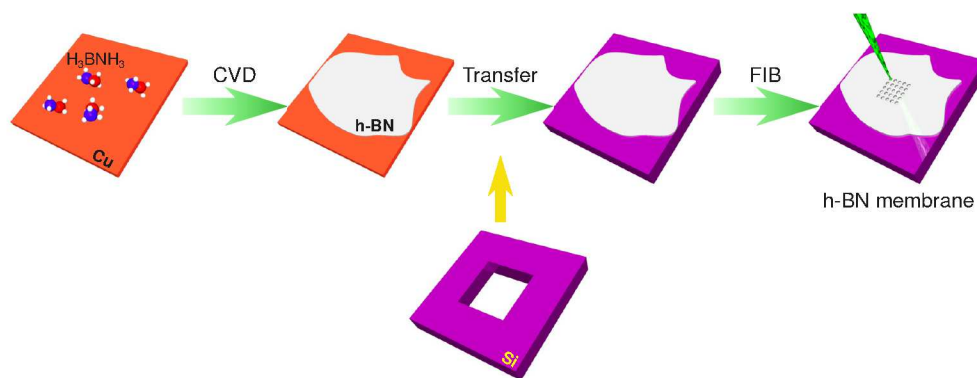


Fig. 1 Fabrication process of h-BN membranes. h-BN is first grown on copper foils, the copper is then etched in an ammonium persulfate solution. The floating h-BN film is transferred onto a hollow silicon substrate and patterned by FIB.

nanochannels. We preferred to grow h-BN film with a thickness of about 100 nm by chemical vapor deposition (CVD)^{24,25} instead of using classical technique like spin or dip-coating with polymer derived ceramics technique,²⁶ better fitted for thicker films.²⁷ To our knowledge, there are only three studies related to h-BN patterning, they are all concerning mono or very few atomic layers of h-BN. Two articles^{7,28} present unreproducible unique nanopores etched by the focused electron beam of a transmission electron microscope (TEM) on a device used for DNA translocation. The third interesting study²⁹ probes the size limitation for a unique nanopore etched by FIB on a h-BN membrane but the resulting sample is not designed for nanofluidic applications. In this work, we show for the first time a complete process for producing nanochannels arrays in h-BN thin films (Fig. 1) supported by substrates designed specifically for fluidic experiments.

h-BN thin film was grown by ambient pressure chemical vapor deposition on Cu foil (25 μm thick, 99.8%, Alfa Aesar). Ammonia-borane (97%, Sigma Aldrich) sublimated at 150 $^{\circ}\text{C}$ was used as precursor. The growth temperature was 1000 $^{\circ}\text{C}$ under a 500 sccm N_2/H_2 flux. Copper was etched away in a $(\text{NH}_4)_2\text{S}_2\text{O}_8$ solution of 5×10^{-2} mol/L concentration and the h-BN film was directly transferred onto a substrate (300 mesh Cu TEM grid, Si or Si/SiN membrane) using a resist-free technique³⁰ adapted for h-BN. A Zeiss NVision 40 FIB/SEM was used to pattern h-BN membranes in spot mode, the Ga^+ beam is held at a point of the sample during the irradiation time (t) or, in a lithography mode to tailor more complex shapes, a predefined pattern is scanned by the FIB, piloted by the software FIBICS. TEM images were recorded in a JEOL JEM 2100F microscope and complementary scanning electron microscopy (SEM) images taken in a Hitachi S-800. Raman spectra were acquired in a Renishaw RM 1000 spectrometer equipped with a 1800 lines/nm grating, using an excitation wavelength of 532 nm and a $\times 50$ objective.

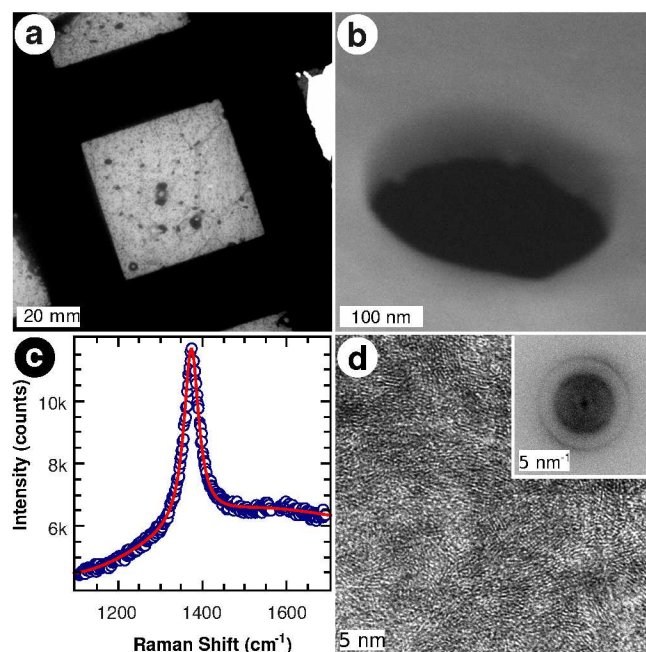


Fig. 2 Characterization of h-BN membranes. (a) SEM micrograph of a h-BN film transferred onto a TEM grid. (b) SEM micrograph of a leaky h-BN film tilted at 54° with respect to the electron beam. (c) Raman spectrum of the h-BN film (blue circles) fitted with a fourth order polynomial and a Lorentzian curve (red line). (d) TEM image of the surface of the h-BN membrane. Inset is a the fast Fourier transform (FFT) of the direct image.

Transferred onto a 300 mesh Cu TEM grid, the film is suspended over the $50 \mu\text{m} \times 50 \mu\text{m}$ windows of the grid (Fig. 2a). A hole in the membrane, observed with the SEM at a tilt angle of 54° (see Fig. 2b) indicates that the film is 120 nm thick. The Raman spectrum of Fig. 2c is typical of the spectra recorded on h-BN films transferred on four distinct Si substrates. The average full width at half maximum and Raman Shift are 45 and 1375 cm^{-1} respectively, indicating a polycrystalline h-BN film with a crystal size of *c.a.* 4 nm.^{31–33} The high resolution TEM image and its FFT (Fig. 2d) confirm the polycrystalline structure of the films.

Their patterning using FIB in spot mode are presented in Fig. 3a for irradiation times ranging from 10 ms to 20 s with an ionic current of 10 pA. The membrane is altered but not completely etched using an operating time inferior to 250 ms. For $t = 250 \text{ ms}$, the hole has an irregular shape with dimensions ranging from 18 to 30 nm (Fig. 3b). The channels diameter is increasing for $250 \text{ ms} \leq t \leq 10 \text{ s}$, following a power law of $V = At^\gamma$, V being the etched volume, A and γ are the fit parameters. $A = 2700 \text{ nm}^3 \cdot \text{s}^{-1}$ and $\gamma = 0.6$. For $t \geq 10 \text{ s}$, the channel diameter is rather constant around 150 nm. Concerning Ga contamination, an energy X-ray dispersive (EDS) spectrum (see Fig. S2) show a very low amount of Ga around the holes (0.1 to 0.5, atomic percentage). The channels are quite stable under air exposure, a slight increase of their diameter may be explained by the presence of Ga and air exposure.³⁴

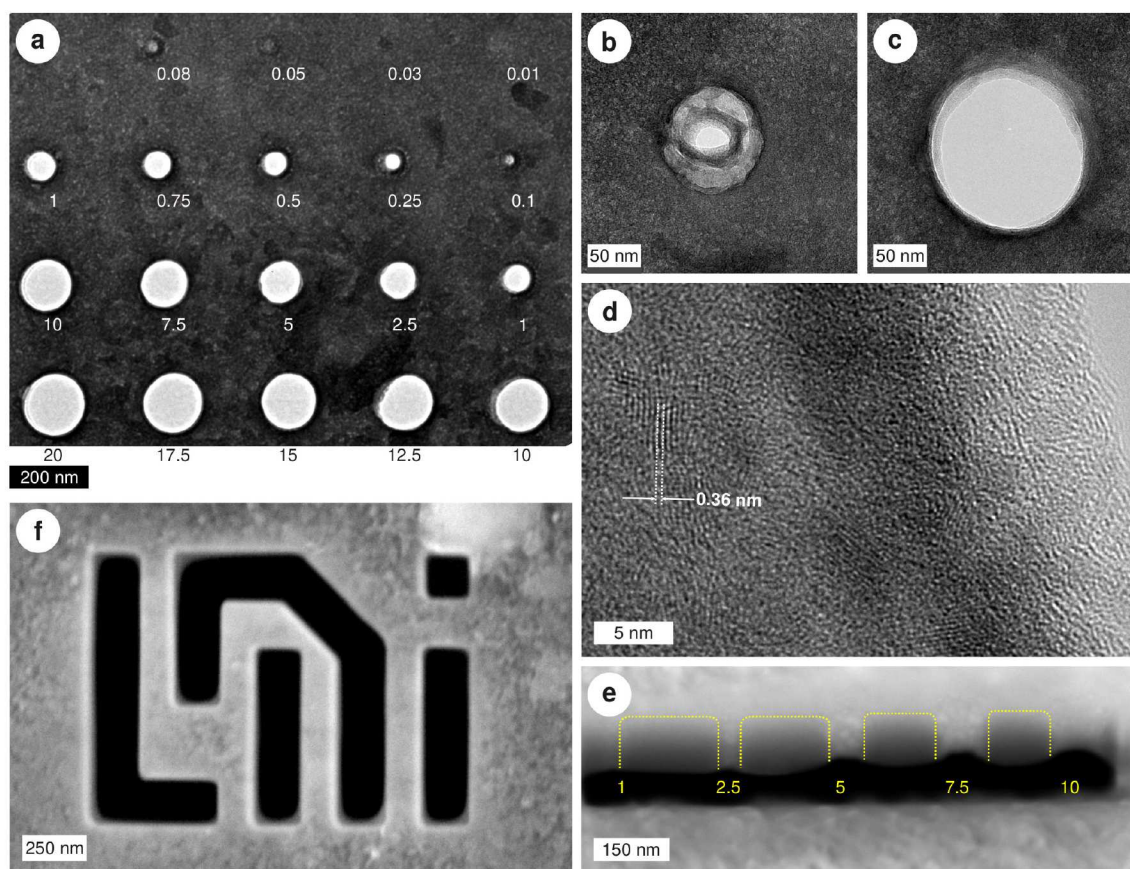


Fig. 3 FIB patterning of h-BN films. (a) Spot mode irradiation with a 10 pA ion beam, irradiation time (s) is indicated below each holes. (b), (c) TEM images of holes shown in (a), etched with 0.25 and 10 s respectively. (d) High resolution TEM image of the edge of the hole shown in (c). (e) SEM image of channels, irradiation times (s) are indicated below each channels. The Channels have been cut through their diameter using FIB. (f) "LMI", the logo of the laboratory patterned using FIB in the lithography mode.

TEM images of the smallest holes (Fig. 3b) shows an area partially etched where material gets redeposited on the walls of the channels. High resolution TEM (Fig. 3d) shows that this area is amorphous. Small h-BN crystallites can be distinguished close to the wall of the channel at 10 to 20 nm, this is probably due to the well known amorphization by the Gaussian profile of the ion beam. Note that this amorphized area disappeared at $t = 10$ s (Fig 3).

In order to reveal the channels of these holes, a series of holes was etched using t between 1 and 10 s, a rectangle was then etched, one side aligned with the centers of the holes. A SEM image (Fig. 3e) has then been taken with a tilted sample. These channels appear to be straight all along the membrane thickness. This is of main importance to ensure the regular liquid flow for further nanofluidic measurement. The SEM image in Fig. 3f evidence that it is possible to etch an arbitrary pattern using this technique opening the way for studying the behavior of arbitrary channels array.³⁵ Since FIB patterning of h-BN membrane produces channels with a regular cylinder shape of various diameter for irradiation times higher than 1 s it seems possible to envisage devices with high density of nano-channels. For that, we have chose $t = 1$ s to produce these particular h-BN membranes.

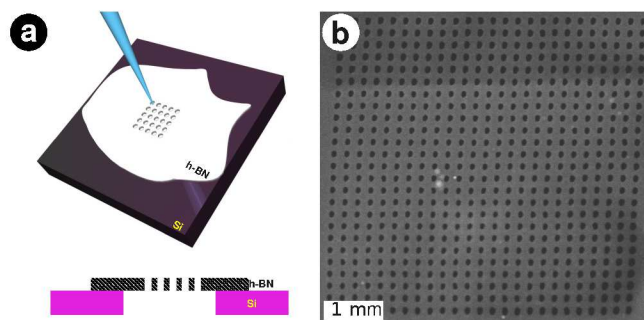


Fig. 4 (a) Schematics presenting the membrane being etched by FIB. (b) SEM image of the device schematized in (a), the h-BN membrane was patterned by a 10 pA FIB.

The substrate used to support the h-BN film is a silicon chip that presents a hollow window ($30 \times 30 \mu\text{m}^2$ square) in its center. A h-BN film was transferred onto that substrate to completely cover this window (Fig. 4a). For the study of nanofluidic properties, this sample aims to separate two aqueous media by forcing the liquid exchange through the channels etched in the h-BN membrane. Each hole of the 25×25 square array shown in Fig. 4b has a diameter of 70 to 80 nm with a hole density of $1.6 \times 10^{11} \text{ cm}^{-2}$. A high density array of nanochannels in a h-BN film has been etched using FIB, nevertheless, concerning the large scale application of this technique, even if the etching time is reduced to 0.5 s per channel, etching 1 mm^2 membrane with a channel density of 10^9 cm^{-2} would last 14 hours. Although this technique can not be applied to the industrial scale, it constitutes a significant technological breakthrough from the unique and unreproducible single nanotube technique. FIB based prototype is of great interest to study the behavior of these h-BN membranes in terms of channel diameter, density or length for nanofluidic experiments. To understand nanofluidic properties from numbered channels array is the first and necessary step to the understanding of macroscopic devices.

Conclusions

This work presents for the first time, a complete process to fabricate membranes containing nanochannels in a h-BN thin film. The 100 nm thick film is produced by CVD using ammonia-borane as precursor and a copper foil as substrate. The FIB patterning of these membranes etched channels with diameter ranging from 30 nm to 130 nm, the edges of the smallest holes being amorphized on a length scale of about 10-20 nm.

The process has been applied to a substrate designed for fluidic experiments, an array of holes (70-80 nm in diameter) with a density of $1.6 \times 10^{11} \text{ cm}^{-2}$ was etched in a h-BN membrane, offering promising experiments for future imminent development in nanofluidics through h-BN.

Acknowledgments

The authors gratefully acknowledge the CECOMO (Université Lyon1) for providing access to the Raman spectroscopy facilities, the CT μ (Université Lyon1) for TEM and SEM access and the CLYM (Insa Lyon) for the dual FIB/SEM access. We also thank N. O'TOOLE for its careful reading of the article and M. Maillard for helpful discussions. This work was supported by the Programme d'investissement d'Avenir Lyon Saint-Etienne "PALSE" : project emergent named "Novel perspectives for blue energy harvesting".

References

- 1 B. E. Logan and M. Elimelech, *Nature*, 2012, **488**, 313–319.
- 2 M. A. Shannon, P. W. Bohn, M. Elimelech, J. G. Georgiadis, B. J. Marias and A. M. Mayes, *Nature*, 2008, **452**, 301–310.
- 3 K. Celebi, J. Buchheim, R. M. Wyss, A. Droudian, P. Gasser, I. Shorubalko, J.-I. Kye, C. Lee and H. G. Park, *Science*, 2014, **344**, 289–292.
- 4 F. Fu and Q. Wang, *Journal of Environmental Management*, 2011, **92**, 407–418.
- 5 T. Y. Cath, A. E. Childress and M. Elimelech, *Journal of Membrane Science*, 2006, **281**, 70–87.
- 6 G. M. Church and W. Gilbert, *PNAS*, 1984, **81**, 1991–1995.
- 7 Z. Zhou, Y. Hu, H. Wang, Z. Xu, W. Wang, X. Bai, X. Shan and X. Lu, *Sci. Rep.*, 2013, **3**, 3287.
- 8 N. Ashkenasy, J. Sanchez-Quesada, H. Bayley and M. R. Ghadiri, *Angewandte Chemie International Edition*, 2005, **44**, 1401–1404.
- 9 P. H. Hoang, K.-B. Yoon and D.-P. Kim, *RSC Adv.*, 2012, **2**, 5323–5328.
- 10 B. E. Logan, B. Hamelers, R. A. Rozendal, U. Schröder, J. Keller, S. Freguia, P. Aelterman, W. Verstraete and K. Rabaey, *Environ. Sci. Technol.*, 2006, **40**, 5181–5192.
- 11 L. Guan, K. Suenaga and S. Iijima, *Nano Lett.*, 2008, **8**, 459–462.
- 12 R. Arenal, P. Lthman, M. Picher, T. Than, M. Paillet and V. Jourdain, *J. Phys. Chem. C*, 2012, **116**, 14103–14107.
- 13 A. C. Y. Liu, R. Arenal and G. Montagnac, *Carbon*, 2013, **62**, 248–255.
- 14 M. Bechelany, S. Bernard, A. Brioude, D. Cornu, P. Stadelmann, C. Charcosset, K. Fiyat and P. Miele, *J. Phys. Chem. C*, 2007, **111**, 13378–13384.
- 15 V. Salles, S. Bernard, A. Brioude, D. Cornu and P. Miele, *Nanoscale*, 2010, **2**, 215–217.
- 16 D. Golberg, Y. Bando, K. Kurashima and T. Sato, *Scripta Materialia*, 2001, **44**, 1561–1565.
- 17 X. Chen, P. Wu, M. Rousseas, D. Okawa, Z. Gartner, A. Zettl and C. R. Bertozzi, *J. Am. Chem. Soc.*, 2009, **131**, 890–891.
- 18 Y. Chen, J. Zou, S. J. Campbell and G. L. Caer, *Applied Physics Letters*, 2004, **84**, 2430–2432.
- 19 L. H. Li, J. Cervenka, K. Watanabe, T. Taniguchi and Y. Chen, *ACS Nano*, 2014, **8**, 1457–1462.
- 20 C. Y. Won and N. R. Aluru, *J. Am. Chem. Soc.*, 2007, **129**, 2748–2749.
- 21 T. A. Hilder, D. Gordon and S.-H. Chung, *Small*, 2009, **5**, 2183–2190.
- 22 A. Siria, P. Poncharal, A.-L. Biance, R. Fulcrand, X. Blase, S. T. Purcell and L. Bocquet, *Nature*, 2013, **494**, 455–458.
- 23 A. Tseng, *Small*, 2005, **1**, 924–939.
- 24 A. Ismach, H. Chou, D. A. Ferrer, Y. Wu, S. McDonnell, H. C. Floresca, A. Covacevich, C. Pope, R. Piner, M. J. Kim, R. M. Wallace, L. Colombo and R. S. Ruoff, *ACS Nano*, 2012, **6**, 6378–6385.

-
- 25 Y. Shi, C. Hamsen, X. Jia, K. K. Kim, A. Reina, M. Hofmann, A. L. Hsu, K. Zhang, H. Li, Z.-Y. Juang, M. S. Dresselhaus, L.-J. Li and J. Kong, *Nano Lett.*, 2010, **10**, 4134–4139.
- 26 S. Yuan, B. Toury, C. Journet and A. Brioude, *Nanoscale*, 2014, **6**, 7838–7841.
- 27 S. Yuan, S. Benayoun, A. Brioude, O. Dezellus, B. Beaugiraud and B. Toury, *Journal of the European Ceramic Society*, 2013, **33**, 393–402.
- 28 S. Liu, B. Lu, Q. Zhao, J. Li, T. Gao, Y. Chen, Y. Zhang, Z. Liu, Z. Fan, F. Yang, L. You and D. Yu, *Adv. Mater.*, 2013, **25**, 4549–4554.
- 29 A. Hemamouche, A. Morin, E. Bourhis, B. Toury, E. Tarnaud, J. Math, P. Guban, A. Madouri, X. Lafosse, C. Ulysse, S. Guilet, G. Patriarche, L. Auvray, F. Montel, Q. Wilmart, B. Plaais, J. Yates and J. Gierak, *Microelectronic Engineering*, 2014, **121**, 87–91.
- 30 K. S. Kim, Y. Zhao, H. Jang, S. Y. Lee, J. M. Kim, K. S. Kim, J.-H. Ahn, P. Kim, J.-Y. Choi and B. H. Hong, *Nature*, 2009, **457**, 706–710.
- 31 R. J. Nemanich, S. A. Solin and R. M. Martin, *Phys. Rev. B*, 1981, **23**, 6348–6356.
- 32 S. Reich, A. C. Ferrari, R. Arenal, A. Loiseau, I. Bello and J. Robertson, *Phys. Rev. B*, 2005, **71**, 205201.
- 33 R. Arenal, A. C. Ferrari, S. Reich, L. Wirtz, J.-Y. Mevellec, S. Lefrant, A. Rubio and A. Loiseau, *Nano Lett.*, 2006, **6**, 1812–1816.
- 34 P. R. Kidambi, R. Blume, J. Kling, J. B. Wagner, C. Baetz, R. S. Weatherup, R. Schloegl, B. C. Bayer and S. Hofmann, *Chem. Mater.*, 2014, **26**, 6380–6392.
- 35 A. Gadaleta, C. Sempere, S. Gravelle, A. Siria, R. Fulcrand, C. Ybert and L. Bocquet, *Physics of Fluids (1994-present)*, 2014, **26**, 012005.

Graphical abstract.

Nanochannels arrays are tailored in h-BN membranes by focused ion beam for nanofluidic applications.

